

On the Shape of $C_6H_6^+$

R. Lindner,* K. Müller-Dethlefs,† E. Wedum, K. Haber,
E. R. Grant‡

The benzene molecule serves as a benchmark among the aromatic hydrocarbons and has been the subject of numerous experimental and theoretical studies. Despite such intensive investigations, the precise structure of the benzene cation ($C_6H_6^+$) is not known. Now, experiments measuring high-resolution state-to-state threshold photoionization spectra of benzene concretely establish the terms of vibronic levels in the distorted cation that are split by higher order Jahn-Teller coupling between its ${}^2E_{1g}$ electronic ground state and $\nu_6 e_{2g}$ in-plane ring-bending vibrational mode. This assignment, in turn, sets the absolute energy phase of the vibronic pseudorotation in this coordinate and thereby offers a definitive experimental determination of the shape of the benzene cation.

Molecules with electronically degenerate ground states confound conventional notions of molecular shape and the ball-and-stick separability of electronic and internuclear degrees of freedom. Nuclear motions coupled with electronic degeneracy link electronic and vibrational angular momenta to distort symmetric structures and profoundly alter the dynamics of vibration and intramolecular energy redistribution (1–4). Such instances of electronic degeneracy have far-reaching implications for chemistry. For example, coordination compounds of many transition metals, as well as open-shell hydrocarbon radicals and radical cations, commonly possess degenerate or near-degenerate ground-state terms, and in such systems vibronic coupling formally breaks the electronic degeneracy, giving rise to vibronic distortion and fluctuation, both of which can affect chemical reactivity (5).

Benzene is a benchmark molecule among the hydrocarbons and serves as an important prototype for aromatic systems in general. The electronic configuration of the neutral molecule is $\dots a_{2u}^2, e_{1g}^4$, and many researchers have considered the change in structure upon ionization to the doubly degenerate ${}^2E_{1g}$ cation ground state. Electron spin resonance interpretations of the condensed phase suggest static in-plane distortion to an obtuse minimum (which has a local electronic symmetry of B_{3g} in the D_{2h} point group that maintains the z axis in the plane of the molecule) (6). Attempts to determine the lower energy distortion of

the benzene cation by ab initio calculations have produced varied and conflicting results. For example, high-level ab initio MP-2 calculations by Raghavachari *et al.* found the apically acute B_{2g} electronic state to be lower, but this ordering reversed with configuration interaction (7). Kato *et al.* found the B_{2g} electronic state lower by an estimated 240 cm^{-1} (8). More recently, Huang and Lunell have calculated that the B_{3g} state is lower by about 165 cm^{-1} (9), whereas Takeshita has obtained results similar to those of Kato (10).

Direct characterization of cation structure by infrared or microwave spectroscopy has not proven practicable. Photoelectron spectroscopy has provided a coarse view (11, 12), and Takeshita has applied ab initio results to interpret low-resolution photoelectron features in terms of transitions to distinct B_{2g} and B_{3g} modifications of the cation (10). The data, however, are too broad to determine secondary structure in the potential, and interpretation in terms of individual states neglects the global nature of the vibronic coupling problem. New techniques, using zero-kinetic-energy (ZEKE) threshold photoelectron discrimination, offer much higher resolution (13, 14), isolating cation vibronic and even rotational structure (15). Applied to benzene, this spectroscopic method directly addresses the question of modulation of the electronic potential energy surface in the region of the ν_6 conical intersection and definitively resolves the controversy concerning the relative stability of the B_{2g} and B_{3g} configurations.

High-resolution threshold photoionization. We resolved the rotational structure of excited vibrational states in $C_6H_6^+$ by combining high-resolution optical-optical double-resonance laser excitation with delayed pulsed field ionization to precisely distinguish electrons produced very near individual quantum-state detailed ionization thresholds. The apparatus for these experiments used a differentially pumped vacuum system

equipped with a pulsed molecular beam source and a threshold photoelectron spectrometer that used standard ZEKE pulsed-field ionization (ZEKE-PFI) electron optics.

Within the delayed-field-ionization and electron-collection region of the spectrometer, a pulsed beam of benzene, seeded at a concentration of 1 percent in argon, was crossed by the output of two frequency-doubled dye lasers. The first laser was fixed on a specific rovibronic transition from the neutral benzene ground state (S_0) to the first excited singlet state (S_1). The second dye laser scanned the spectrum of transitions from the selected S_1 rotational state to the thresholds for forming accessible rovibrational states of the cation. Each of these thresholds forms a convergence limit for a complete set of Rydberg series. Within a few wave numbers of each limit, Stark mixing in the weak field presented by background ions lengthens the lifetimes of very high Rydberg states. Absorption to these states, detected by delayed pulsed field ionization, marks the position of each threshold and thus determines the spectrum of the internal states of the cation (16).

Rovibrational structure of $C_6H_6^+$. A broad scan of the threshold photoionization spectrum of benzene (Fig. 1) shows the vibronic structure of the cation electronic ground state. Observable in the spectrum are bands at fundamental frequencies characteristic of ν_6 , ν_{16} , ν_4 , and ν_1 . A complete absence of harmonic regularity can be seen at higher energies. A key pair of bands (Fig. 2) falls between the origin and the fundamental of the Jahn-Teller active mode, ν_6 . As discussed below, vibronic analysis establishes this pair of bands as the B_{1g} and B_{2g} components of the ν_6 fundamental, driven to lower energy by linear Jahn-Teller coupling. The spectrum shown is produced by a scan from the $6^1 J' = 2, K' = 2, -l$ resolved rotational level of the S_1 state, where J' , K' , and l refer to total angular momentum, its molecule-fixed projection, and vibrational angular momentum, respectively. Its structure is readily fit by a Hamiltonian incorporating rotational constants that match those fit to spectra originating from higher intermediate rotational states. Unique to this set of transitions, however, is the fact that it shows sub-bands terminating on states with rotational angular momentum projections $K^+ = 0$ that display only half the expected rotational lines. As indicated by ladders in Fig. 2, odd final values of N^+ are apparently absent in the lower energy band, whereas even N^+ levels are missing in the higher energy component.

Vibronic potential energy. The vibronic spectrum of $C_6H_6^+$ (Fig. 1) is characterized by intense transitions to levels of

R. Lindner and K. Müller-Dethlefs are in the Institut für Physikalische und Theoretische Chemie, Technischen Universität München, D-85748 Garching, Germany. E. Wedum, K. Haber, and E. R. Grant are in the Department of Chemistry, Purdue University, West Lafayette, IN 47907, USA.

*Present address: Radiant Dyes Laser GmbH, Friedrichstrasse 58, D-42929 Wermelskirchen, Germany.

†Present address: Department of Chemistry, University of York, Heslington, York YO15DD, UK.

‡To whom correspondence should be addressed.

low vibrational frequency that are not present in the neutral molecule. Harmonic progressions are not in evidence, and the higher energy portion of the spectrum is very irregular, exhibiting a dense system of vibronically active states. The source of this irregularity and spectroscopic activity can be readily understood in terms of the well-recognized vibronic coupling between the E_{1g} electronic state of the cation and its degenerate vibrational modes. This problem has been addressed theoretically by a number of researchers, with most recent calculations pointing to a multiple-möde, multiple-electronic-state character of the coupling at higher vibrational excitation (17). Much of the complexity of the vibrational problem, however, is well represented by the behavior of the lower frequency modes, and the more qualitative issue of the shape of cation ground state invites a simpler approach.

The lowest active mode is in-plane C-C-C ring bending, ν_6 . Distortion in this coordinate produces the planar acute and obtuse D_{2h} structures considered in theoretical treatments of the cation geometry (18). Analyses of the low-resolution photoelectron spectrum (12) and of the cation-core vibronic structure exhibited by higher Rydberg states (19) establish this mode as the main carrier of vibronic intensity in the first 1000 cm^{-1} . Thus, our analysis of the spectrum and its implications for stable cation geometries centers on this ring-bending coordinate and treats the Jahn-Teller coupling as a single mode problem.

Even restricted to a single mode, Jahn-Teller distortion of the vibrational potential readily predicts irregularity in the low-frequency spectrum. A two-dimensional diabatic basis of electronic states, in which the nuclear kinetic energy is diagonal, yields a vibrational Hamiltonian in terms of electronic matrix elements. These can be expanded in a Taylor series to the second order about a reference configuration, the natural choice being the one of highest symmetry, to yield the standard result (1, 4, 20)

$$\begin{bmatrix} \frac{1}{2} \rho^2 + \frac{1}{2} P_\rho^2 + \frac{1}{2\rho^2} P_\phi^2 & k\rho e^{-i\phi} + \frac{1}{2} g\rho^2 e^{2i\phi} \\ k\rho e^{i\phi} + \frac{1}{2} g\rho^2 e^{-2i\phi} & \frac{1}{2} \rho^2 + \frac{1}{2} P_\rho^2 + \frac{1}{2\rho^2} P_\phi^2 \end{bmatrix} \quad (1)$$

where ρ and ϕ describe vibrational amplitude and phase in dimensionless polar coordinates, respectively, and k and g are the linear and quadratic vibronic coupling coefficients. The diagonal elements represent the two isotropic harmonic potentials of the undistorted degenerate electronic state, whereas nonzero off-diagonal elements give the coordinate-dependent vibronic coupling terms, which distort the adiabatic potential and alter the regular spacing of vibrational levels.

Neglecting the nuclear kinetic energy terms, P_ρ and P_ϕ , and treating the vibrational coordinates as parameters, we can easily diagonalize Eq. 1 to obtain the adiabatic vibrational potential energy surfaces for a single Jahn-Teller active mode:

$$E(\rho, \phi) = \frac{1}{2} \rho^2 \pm k\rho \left[1 + \frac{g\rho}{k} \cos(3\phi) + \frac{g^2 \rho^2}{4k^2} \right]^{1/2} \quad (2)$$

For small values of g/k , the potential at low amplitude simplifies to

$$E(\rho, \phi) = \frac{1}{2} [\rho^2 \pm g\rho^2 \cos(3\phi)] \pm k\rho \quad (3)$$

This solution yields the familiar "sombbrero" structure of the single-mode conical intersection, where k determines the depth (D) of the distorted minimum in relation to the symmetric intersection point according to $D = 1/2k^2$, and g modulates the potential as a function of the phase of the distortion.

That Jahn-Teller coupling can produce irregularity in the vibrational spectrum is clear from this potential. When coupling is zero, the potential offers the well-defined restoring

forces and regular level structure of the isotropic two-dimensional harmonic oscillator. However, even weak linear coupling substantially alters vibrational restoring forces. The potentials are nested, and it is no longer obvious to which surface the vibrational motion should respond. Only in the limits of large linear coupling and vibrational energy substantially below that of the conical intersection can we imagine vibrational motion with any regularity. Here, distortion forces modify the nature of vibration to consist of radial oscillation in ρ about a nonzero ρ_0 , combined with an internal rotation through all phases of the normal coordinates that span the degenerate vibrational mode (21). As apparent in Eq. 3, finite values of g produce a threefold barrier to this rotation, placing minima at values of ϕ equal to

$$\left\{ 0 \frac{2\pi}{3} \frac{4\pi}{3} \right\} \text{ or } \left\{ \frac{\pi}{3} \pi \frac{5\pi}{3} \right\}$$

depending on the sign of g . To completely characterize the structural consequences of Jahn-Teller coupling in the benzene cation, it is essential that we understand this feature of the vibronic potential.

Vibronic energy levels. The characterization of vibronic coupling in terms of its effects on coordinate-dependent electronic energy is a familiar problem in electronic structure theory. Experiments, however, do not directly measure potential energy surfaces. Instead, by cataloging spectroscopic positions, experimental measurements return eigenvalues corresponding to the stationary

Fig. 1. Low-resolution ZEKE-PFI threshold photoionization spectrum of benzene observed in transitions from the 6^1 level of the first excited singlet state of the neutral molecule, showing the vibronic structure of the cation ground electronic state.

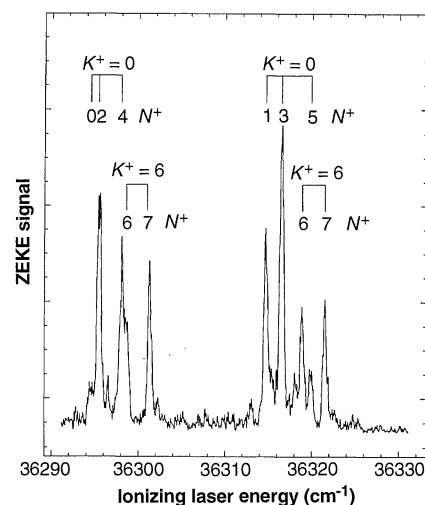
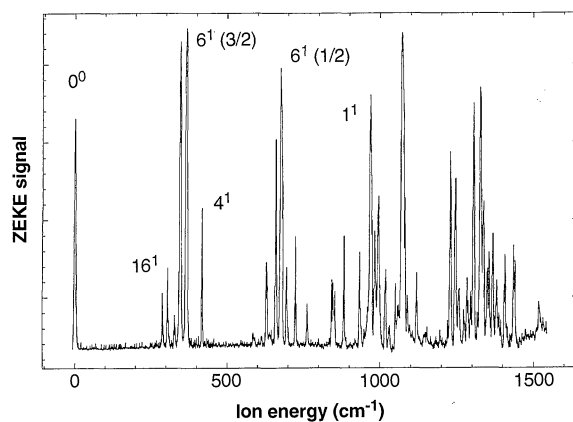


Fig. 2. High-resolution ZEKE-PFI threshold photoionization spectrum of benzene in the region 350 cm^{-1} above the adiabatic threshold observed in transitions from the single selected rotational state $J' = 2, K' = 2, -/$ of the 6^1 level in the first excited singlet state of the neutral molecule. We sharpened the resolution by using stepped-pulse field ionization (16). Rotational structure associated with these transitions was assigned according to the ladders presented above each band.

states of those potentials. It is therefore important to take the model beyond potentials to obtain theoretical eigenvalues for comparison to experiment.

To achieve this, it is necessary to include the nuclear kinetic energy and diagonalize in a basis of isotropic two-dimensional harmonic oscillator eigenfunctions of the uncoupled Hamiltonian. Solutions give the vibronic energy levels and wave functions, sorted on the basis of a half-odd integral quantum number, j , consistent with the double-valued electronic eigenstates of Eq. 1. For finite linear-plus-quadratic coupling, the problem block factors according to $j' = j \bmod 3$.

Figure 3 shows the results in the form of a correlation diagram in k for $g = 0$. The ground state is doubly degenerate, with term symmetry E_{1g} . The first Jahn-Teller excited state (6^1 in our single-mode model for $C_6H_6^+$) is vibronically fourfold degenerate in the limit of zero coupling. With increasing values of k , this quartet of excited states splits to form a doubly degenerate radial oscillator level, E_{1g} $6^1(j' = 1/2)$, and a pair of excited pseudorotation levels, B_{1g} $6^1(3/2)$ and B_{2g} $6^1(3/2)$, which for zero g remain accidentally degenerate. A vertical dashed line on the correlation diagram indicates values of k (0.88) and of harmonic frequency, ω (536 cm^{-1}), that center corresponding eigenvalues on positions assigned experimentally for these bands. With the inclusion of finite quadratic coupling ($g = 0.02$), computed $6^1(3/2)$ positions split to fit with the fine structure observed experimentally in the region 350 cm^{-1} above the origin.

Energy ordering of the $6^1(3/2)$ states and phase of the vibronic pseudorotation potential. The correlation diagram in Fig. 3 identifies the states that appear in the spectrum at a cation energy of 350 cm^{-1} as the pair of pseudorotation levels B_{1g} , B_{2g} $6^1(3/2)$ split by nonzero quadratic coupling. This fit to the vibronic spectrum, however, does not assign the order of these terms. A high-resolution ZEKE scan (Fig. 2) shows a distinctive rotational structure for transitions in this system that terminate on levels with $K^+ = 0$. In the lower energy component of the doublet, only levels for which N^+ is even appear, whereas the upper component shows transitions only to levels for which N^+ is odd. The cause for this difference can be established by considering the nuclear-spin statistical weights of the individual rotational levels in states with vibronic symmetry B_{1g} and B_{2g} .

In the molecular point group D_{6h} , the symmetry species of the rovibronic states with projections $K = 0$ alternate dependence on the total angular momentum quantum number. For a state with vibronic symmetry B_{1g} , levels for which N is even have rovibronic symmetry B_{1g} , whereas those levels for which N is odd have rovibronic symmetry B_{2g} . In a state with vibronic symmetry B_{2g} , this order is reversed. For benzene, Fermi-Dirac nuclear-

spin statistics permit only those wave functions with total symmetry B_{1g} , where the symmetry of the total wave function is determined by the product of the rovibronic symmetry with that of the nuclear-spin wave function.

The 2^6 nuclear-spin wave functions of benzene span a reducible representation of the D_{6h} point group with a decomposition $\Gamma_{ns} = 13A_1 + A_2 + 7B_1 + 3B_2 + 9E_1 + 11E_2$ (22, 23). To conform with the requirements of nuclear-spin statistics, rovibronic states with symmetry species B_{1g} must have a nuclear-spin symmetry of A_1 , whereas those with rovibronic symmetry B_{2g} must have a nuclear-spin symmetry of A_2 . Considering nuclear-spin degeneracy factors, states with rovibronic symmetry B_{1g} will be 13 times more abundant than states with rovibronic symmetry B_{2g} .

In the spectrum in Fig. 2, the positions of the missing lines are indeed marked by weak structure. The strong (B_{1g}) lines in the lower component are even. This unambiguously assigns that state the vibronic symmetry B_{1g} . In the upper component, the lines with rovibronic symmetry B_{1g} correspond to odd values of N , establishing that state as vibronically B_{2g} . Rotational structure in the ZEKE spectrum thus directly determines the energy ordering of the quadratically split $6^1(3/2)$ levels of the benzene cation as B_{2g} above B_{1g} .

Sign of g and the phase of the vibronic pseudorotation. A relation between the sign of g and the energy ordering of the levels can be established by examining coefficients $a_{vl\Lambda}$ in the vibronic eigenvectors of Eq. 1, which have the form

$$\begin{aligned} \vartheta(\phi) &= \sum_{\pm} \Lambda \sum_{l > 0} a_{vl\Lambda} |v l \Lambda\rangle \\ \vartheta^*(\phi) &= \sum_{\pm} \Lambda \sum_{l < 0} a_{vl\Lambda} |v l \Lambda\rangle \end{aligned} \quad (4)$$

where the basis functions are defined in terms of vibrational angular momentum, l , and electronic angular momentum, Λ , and transform under the operations of the D_{6h} point group according to

$$|v l \Lambda\rangle \propto z e^{i(2l \pm 1)\phi} \quad (5)$$

The D_{6h} projection operators establish eigenvector symmetries for these 2π periodic eigenfunctions of the $E_{1g} \otimes e_{2g}$ Hamiltonian according to

$$\begin{aligned} P^{B_{1g}}(|v l \Lambda\rangle) &= \sum_{R \in D_{6h}} \chi_R^{B_{1g}} \\ R(|v l \Lambda\rangle) &= \vartheta + \vartheta^* \end{aligned} \quad (6)$$

and

$$\begin{aligned} P^{B_{2g}}(|v l \Lambda\rangle) &= \sum_{R \in D_{6h}} \chi_R^{B_{2g}} \\ R(|v l \Lambda\rangle) &= \vartheta - \vartheta^* \end{aligned} \quad (7)$$

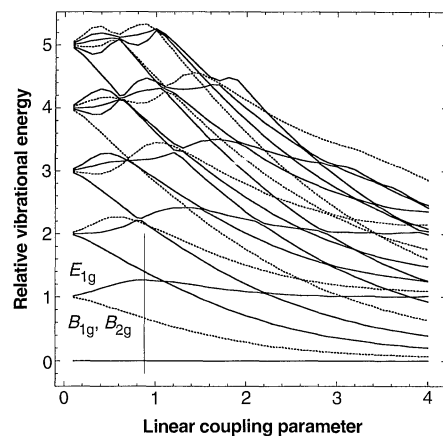


Fig. 3. Correlation diagram showing the level structure of the single-mode linear Jahn-Teller problem ($g = 0$) as a function of the linear coupling parameter k . Vibrational energy and k are presented in reduced units in which the vibrational frequency is 1.

where $\chi_R^{B_{1g}}$ is the character of symmetry operation R belonging to the irreducible representation B_{1g} . Following a similarity transformation of Eq. 1 (24) and diagonalization in the symmetrized basis, we find for $g > 0$ that the lowest eigenvector in the $j' = 3/2$ block transforms according to Eq. 5 and thus conforms with a vibronic symmetry of B_{1g} . Therefore, the ordering established experimentally, B_{1g} below B_{2g} , fits with the solution for positive values of g (relative to k). This places the three minima at the normal coordinate phase angles

$$\phi = \left\{ 0, \frac{2\pi}{3}, \frac{4\pi}{3} \right\}$$

but leaves a Cartesian reference for the pseudorotation phase, as well as the local electronic structure at the distorted minimum energy geometry, as yet undefined.

Cartesian phase of the threefold minimum. In a model that confines higher order coupling to v_6 , the global minimum energy configuration of $C_6H_6^+$ will correspond to one of two ring-bent D_{2h} structures obtained by linear combination of displacements in this doubly degenerate normal mode. The qualitative structure, acute or obtuse with respect to C-C-C apical angles, and the local electronic configuration within the minimum correlate smoothly from very weak coupling to strong. In the strong coupling limit, quadratic wells in the pseudorotation trough trap a threefold, near-degenerate ground state composed of the D_{6h} degenerate ground state plus the lower member of the $6^1(3/2)$ doublet, separated by the pseudorotation tunneling frequency. The vibronic symmetries of these levels in strong coupling must reflect the local electronic symmetry of the well. Thus, correlating back, the experimental spectroscopic level structure ob-

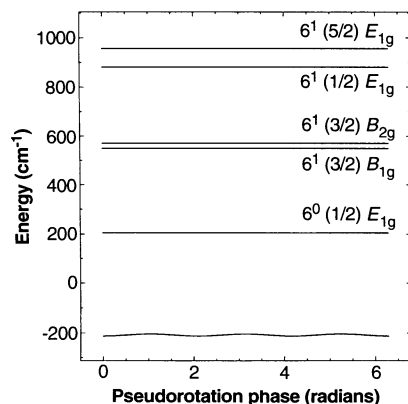


Fig. 4. Diagram showing the energy of the zero point and the first few excited vibrational levels in the ν_6 normal coordinate compared with the modulation of the radial minimum of the potential energy surface as a function of phase angle in the pseudorotation coordinate.

served under weak or even very weak coupling conditions must signify the Cartesian phase of the quadratic modulation.

These results experimentally establish the vibronic symmetries for the levels constituting this triad in D_{6h} : E_{1g} and B_{1g} . Distorting to a local D_{2h} symmetry while retaining the z axis in the plane of the molecule yields correlating vibronic levels, $B_{2g} + B_{3g}$ and B_{2g} , respectively. This experimental set is to be compared with zero-point vibronic symmetries derived from threefold minima possessing either of the possible local D_{2h} electronic terms, B_{2g} or B_{3g} .

This reduction must be viewed with care, however, because for a conical intersection, Berry's phase (25) requires a vibronically degenerate ground state (26). A resolution of this apparent conflict can be found in recent work by Zwanziger and Grant (20), which shows that quadratic coupling introduces three additional intersections. These lie on a radius $\rho = 2k/g$, which marks a sharp transition between Jahn-Teller behavior, characterized by half-odd integral angular momentum (degenerate ground state), and Renner-Teller behavior with integral angular momentum (nondegenerate ground state). Thus, carrying the correlation to sufficiently large values of g , one encounters a limit in which the three outer degenerate points on the potential lie close to the origin and which thus must play a role in defining the topological phase of any adiabatically separable evolution of the vibrational phase. With evolution about all four intersections, the associated geometric phase is even, and the appropriate correlation limit for the ground state is nondegenerate.

Under such circumstances, it is justifiable to construct the vibronic levels of the threefold minimum by first distorting the molecule in normal coordinates of ν_6 to a

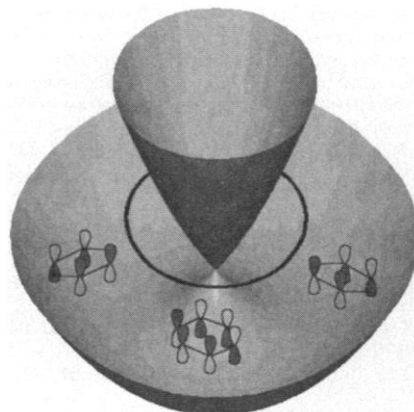


Fig. 5. A three-dimensional view of the potential surface (Eq. 3) in the normal coordinate space of ν_6 , with a Cartesian representation of the pseudorotation at the energy of the zero point, including nodal patterns for the highest occupied molecular orbitals in the pseudorotation sequence: acute (B_{2g}), obtuse (B_{3g}), and acute (B_{2g}).

D_{2h} configuration and then applying the local electronic symmetry of the minimum. Correlation of the first two pure vibrational levels from D_{6h} to D_{2h} yields $a_g + a_g + b_{1g}$. A direct product with B_{3g} , the local term for an obtuse minimum, gives $B_{2g} + B_{3g} + B_{3g}$, which does not agree with the structure observed experimentally. Multiplication by the B_{2g} term of the acute minimum, on the other hand, gives $B_{2g} + B_{2g} + B_{3g}$, which fits with the experimental splitting. We thus conclude that the experimental ordering of the quadratically split $6^1 (3/2)$ states, B_{1g} beneath B_{2g} , demands a distorted benzene cation structure with a locally B_{2g} (acute) global minimum.

We reach the same conclusion if we construct the zero-point triad by taking linear combinations of Gaussian functions centered on the threefold minima in the pseudorotation coordinate ϕ . This procedure yields a pair of pure vibrational states—one of which is doubly degenerate and the other of which is totally symmetric—displaced by the tunneling interaction. By its vibronic term, this split component thus directly reflects the local electronic symmetry of the pseudorotation well. Rotational structure establishes that the vibronic symmetry of the split component of the ground-state triad in this case is B_{1g} , which correlates to B_{2g} in D_{2h} symmetry, thus directly indicating a B_{2g} local minimum.

The shape of $C_6H_6^+$. The magnitude of the coupling parameters derived from the fit of the computed positions to the experimental spectrum provides an important added perspective. From k and ω , we can calculate the amplitude and energy of the distortion—that is, $\rho_0 = 0.12 \text{ \AA}$ and $D = \omega k^2/2 = 208 \text{ cm}^{-1}$. For $\phi = 0$, assuming no C–C bond displacement, this corresponds

to a C–C–C angle of 118.1 degrees. The cation is definitely distorted by linear Jahn-Teller coupling in ν_6 , but the effect of quadratic coupling is very small (Fig. 4). From rotational intensities in the spectrum, we know that the wells in the pseudorotation coordinate correspond with local B_{1g} electronic configurations (B_{2g} in D_{2h} symmetry), whereas the saddle points are locally B_{2g} (B_{3g} in D_{2h}). The energy difference between these stationary points on the potential provides a barrier to pseudorotation. For the coupling parameters that fit the vibronic structure of $C_6H_6^+$, however, this modulation amounts to only 8 cm^{-1} . This small barrier is far less than the 413 cm^{-1} zero-point energy in ν_6 alone. The zero-point energy in fact lies above the point of intersection. Figure 5 shows a three-dimensional view of the potential surface in the normal coordinate space of ν_6 , with a Cartesian representation of the pseudorotation at the energy of the zero point. Obviously, the vibrational wave function of the benzene cation ground state will remain largely unaffected by such a small deviation of the potential from cylindrical symmetry. Thus, there seems little cause to view $C_6H_6^+$ in terms of D_{2h} structures with locally nondegenerate electronic configurations.

In summary, examination of patterns apparent in rotationally resolved threshold photoionization spectra resolves a decades-old question on the shape of the benzene cation. Absolute vibronic symmetries assigned to bands split by quadratic coupling establish that the global minimum is acute D_{2h} . Complete analysis of the vibronic spectrum, however, further shows that the energy difference between distortion isomers on the pseudorotation coordinate are no greater than a few percent of the zero-point energy in that coordinate alone. Thus, the search for the shape of $C_6H_6^+$ now leads not to a pronouncement on structure, but to the realization that the cation is fluxional, dynamically coupled, and necessarily viewed in D_{6h} symmetry.

REFERENCES AND NOTES

- H. C. Longuet-Higgins, *Adv. Spectrosc.* **2**, 429 (1961).
- A. D. Liehr, *Annu. Rev. Phys. Chem.* **13**, 41 (1962); *J. Phys. Chem.* **67**, 389 (1963); *ibid.*, p. 471.
- H. Köppel, W. Domcke, L. S. Cederbaum, *Adv. Chem. Phys.* **57**, 59 (1984).
- R. L. Whetten, G. S. Ezra, E. R. Grant, *Annu. Rev. Phys. Chem.* **36**, 277 (1985).
- I. B. Bersuker, *The Jahn-Teller Effect and Vibronic Interactions in Modern Chemistry* (Plenum, New York, 1984).
- M. Iwasaki, K. Toriyama, K. Nunome, *J. Chem. Soc. Chem. Commun.* (1983), p. 320.
- K. Raghavachari, R. C. Haddon, T. A. Miller, V. E. Bondebey, *J. Chem. Phys.* **79**, 1387 (1983).
- H. Kato, K. Hirao, M. Sano, *J. Mol. Struct.* **104**, 489 (1983).
- M. Huang and S. Lunell, *J. Chem. Phys.* **92**, 6081 (1990).
- K. Takeshita, *ibid.* **101**, 2192 (1994).

11. A. W. Potts, W. C. Price, D. G. Streets, T. A. Williams, *Faraday Discuss. Chem. Soc.* **54**, 168 (1972).
12. S. R. Long, J. T. Meek, J. P. Reilly, *J. Chem. Phys.* **79**, 3206 (1983).
13. See, for example, K. Müller-Dethlefs, M. Sander, E. W. Schlag, *Z. Naturforsch. A* **39**, 1089 (1984); K. Müller-Dethlefs and E. W. Schlag, *Annu. Rev. Phys. Chem.* **42**, 109 (1991); K. Müller-Dethlefs, E. W. Schlag, E. R. Grant, K. Wang, B. V. McKoy, *Adv. Chem. Phys.* **90**, 1 (1995).
14. R. Lindner, B. Beyl, H. Sekiya, K. Müller-Dethlefs, *Angew. Chem. Int. Ed. Engl.* **32**, 603 (1993); R. Lindner, H. Sekiya, K. Müller-Dethlefs, *ibid.*, p. 1364.
15. K. Müller-Dethlefs, M. Sander, E. W. Schlag, *Chem. Phys. Lett.* **112**, 291 (1984); L. A. Chewter, M. Sander, K. Müller-Dethlefs, E. W. Schlag, *J. Chem. Phys.* **86**, 4737 (1987).
16. A delay of several microseconds served to discriminate against prompt electrons produced by direct photoionization processes. A slow-rising, stepped-field ionization pulse was used to allow time-of-flight discrimination of electrons, which were formed from long-lived, high-Rydberg states that fall within a very narrow band of binding energies. This technique provided a resolution of relative energies better than 0.5 cm^{-1} . See R. Lindner, H. J. Dietrich, K. Müller-Dethlefs, *Chem. Phys. Lett.* **228**, 417 (1994).
17. J. Eiding, R. Schneider, W. Domcke, H. Köppel, W. von Niessen, *Chem. Phys. Lett.* **177**, 345 (1992); J. Eiding and W. Domcke, *Chem. Phys.* **163**, 133 (1992).
18. K. Raghavachari, R. C. Haddon, T. A. Miller, V. E. Bondybey, *J. Chem. Phys.* **79**, 1387 (1983).
19. R. L. Whetten, K. S. Haber, E. R. Grant, *ibid.* **84**, 1270 (1986).
20. J. W. Zwanziger and E. R. Grant, *ibid.* **87**, 2954 (1987).
21. J. Schön and H. Köppel, *ibid.* **102**, 9292 (1995).
22. A. Weber, *ibid.* **73**, 3952 (1980).
23. K. Balasubramanian, *ibid.* **74**, 6824 (1981).
24. E. Wedum, thesis, Purdue University (1994).
25. M. V. Berry, *Proc. R. Soc. London Ser. A* **392**, 45 (1984).
26. F. S. Ham, *Phys. Rev. Lett.* **58**, 725 (1987).
27. K.M.-D. and R.L. gratefully acknowledge support from the Deutsche Forschungsgemeinschaft and the Commission of the European Union. Contributions by E.R.G., K.H., and E.W. were supported by a grant from the National Science Foundation (CHE-9307131). E.R.G. also thanks H. Köppel for helpful discussions and gratefully acknowledges the Alexander von Humboldt Foundation for a U.S. Senior Scientist Award and E. W. Schlag for generous hospitality, which made this collaborative effort possible.

15 November 1995; accepted 29 January 1996

AAAS–Newcomb Cleveland Prize

To Be Awarded for a Report, Research Article, or an Article Published in *Science*

The AAAS–Newcomb Cleveland Prize is awarded to the author of an outstanding paper published in *Science*. The value of the prize is \$5000; the winner also receives a bronze medal. The current competition period began with the 2 June 1995 issue and ends with the issue of 31 May 1996.

Reports, Research Articles, and Articles that include original research data, theories, or syntheses and are fundamental contributions to basic knowledge or technical achievements of far-reaching consequence are eligible for consideration for the prize. The paper must be a first-time publication of the author's own work. Reference to pertinent earlier work by the author may be included to give perspective.

Throughout the competition period, readers are

invited to nominate papers appearing in the Reports, Research Articles, or Articles sections. Nominations must be typed, and the following information provided: the title of the paper, issue in which it was published, author's name, and a brief statement of justification for nomination. Nominations should be submitted to the AAAS–Newcomb Cleveland Prize, AAAS, Room 924, 1333 H Street, NW, Washington, DC 20005, and **must be received on or before 30 June 1996**. Final selection will rest with a panel of distinguished scientists appointed by the editor-in-chief of *Science*.

The award will be presented at the 1997 AAAS annual meeting. In cases of multiple authorship, the prize will be divided equally between or among the authors.